VAD Analysis of Nonlinear Wind Fields

D. CAYA AND I. ZAWADZKI

Université du Québec à Montréal, Québec, Canada

(Manuscript received 31 July 1991, in final form 13 December 1991)

ABSTRACT

A critical review of the velocity–azimuth display (VAD) analysis for the retrieval of wind, divergence, and deformation from single-Doppler observations is presented. It is shown that in situations when the linear wind assumption is not valid the VAD analysis leads to incorrect conclusions. The range and height dependence of single-Doppler data contains information on the nonlinearity of the wind field and allows a generalized analysis by which vertical profiles of wind, divergence, and deformation at the radar site can in principle be obtained. These ideas are illustrated by two case analyses of single-Doppler observations in clear air.

1. Introduction

Single-Doppler radar observations of the atmosphere give only one component of the velocity field. To get physically meaningful information from these data, assumptions have to be made either on the spatial or on the temporal dependence of the velocity field. Usually, the assumptions are made on the spatial variations of the wind field rather than on its temporal variation. In particular, the assumption of a wind field linearly varying in space has been widely used (Browning and Wexler 1968; Easterbrook 1973; Waldteufel and Corbin 1979). As shown by Passarelli (1983), this assumption is unduly restrictive. A linear wind field imposes a constant divergence over the scanned region while, in fact, the average divergence over a circle as a function of range can be measured directly without any assumption (Rabin and Zawadzki 1984). The attractive feature of the linearity assumption is its relative conceptual and practical simplicity.

As an introduction, we will present the interpretation of the radial velocity field as made by Browning and Wexler (1968, henceforth to be referred to as BW). They pointed out that, for a linear wind field, the value of the radial velocity V_r (positive away from the radar) observed at fixed values of range and elevation can be expressed as

$$V_r(r, \beta) = \frac{r}{2}(\bar{u}_x + \bar{v}_y) + u_0 \sin\beta + v_0 \cos\beta + \frac{r}{2}(\bar{u}_y + \bar{v}_x)\sin 2\beta + \frac{r}{2}(\bar{v}_y - \bar{u}_x)\cos 2\beta \quad (1.1)$$

where β is the azimuth angle measured from the north. The notation u_x stands for the derivative $\partial u/\partial x$. In this expression, the effects of fall velocity and elevation angle have been neglected. The overbars indicate mean values within the circle of radius r as defined by BW.

On the other hand, if a Fourier expansion up to the second harmonic is made on the radial velocities taken at constant range, V_r can be expressed as

$$V_r(\beta) = a_0 + a_1 \sin\beta + b_1 \cos\beta + a_2 \sin 2\beta + b_2 \cos 2\beta \quad (1.2)$$

where β is the azimuth angle. Finally, a direct comparison of (1.1) and (1.2) leads to a possible interpretation of the Fourier coefficients (hereafter to be called F coefficients) as

$$a_0 = \frac{r}{2}(\bar{u}_x + \bar{v}_y) \quad (1.3)$$

$$a_1 = u_0 \quad (1.4)$$

$$a_2 = \frac{r}{2}(\bar{u}_y + \bar{v}_x) \quad (1.5)$$

$$b_1 = v_0 \quad (1.6)$$

$$b_2 = \frac{r}{2}(\bar{v}_y - \bar{u}_x). \quad (1.7)$$

We see that $2a_0/r$ can be interpreted as the mean divergence, a_1 and b_1 as the values of u and v at the center of the scanned circle, respectively, and $2a_2/r$ and $2b_2/r$ as the mean shearing and stretching deformation, respectively.

In this treatment, a linear wind is assumed in an attempt to reproduce the radial velocities observed at the given range. This linear field is completely specified with six parameters (u_0, v_0, u_x, u_y, v_x, v_y). It is easy

Corresponding author address: Prof. Isztar Zawadzki, Université du Québec à Montréal, Département de Physique, Case postale 8888, Montreal, H3C 3P8 Québec, Canada.

to see from (1.1) that u_y and v_x have exactly the same spatial dependence (in r, β) and, therefore, only five equations are obtained from this analysis. This is the reason that the linear field, used to approximate the real field, cannot be completely determined. Thus, if the actual wind is linear this analysis can provide, at most, the mean divergence, the mean deformation, and the components of the wind at the center of the scanned circle. In this so-called VAD (velocity–azimuth display) analysis, only the azimuthal dependence of the radial velocity is used. The dependence of the radial velocity on range is ignored even if it shows a behavior not compatible with the assumption of linearity.

Let us emphasize that while (1.1) is a model for the airflow, (1.2) is a purely mathematical representation of Doppler measurements not related to any particular hypothesis about the wind field. Thus, the information obtained by the VAD analysis relates to the hypothetical wind field, not to the real wind. In effect, the foregoing derivation of BW proves that the linear spatial dependence of u and v is a sufficient condition for the interpretation of the F coefficients in (1.2) in terms of physically meaningful parameters. The inverse, however, is not true. An infinite set of nonlinear wind fields exists such that two harmonics of the Fourier analysis are sufficient to describe the radial velocity as a function of azimuth at constant range. For example, the purely quadratic field

$$u = u_{xx}x^2 + u_{yy}y^2$$
$$v = 0 \tag{1.8}$$

with the condition $u_{xx} = u_{yy}$ has a radial velocity perfectly represented by (1.2) with $a_0 = b_1 = a_2 = b_2 = 0$ and $a_1 \neq 0$. In this case, however, a_1 will not give the wind at the radar site (which is nil).

Furthermore, since in the VAD analysis only one out of two components of a horizontal wind field is adjusted by a least-squares fit, it is not obvious that the adjusted field will represent the best linear approximation to the actual two-dimensional wind.

In this work we will consider the VAD analysis for a general form of a nonlinear wind. A technique will be suggested by which some parameters of physical importance can be retrieved from single-Doppler data in situations where strong perturbations to a linear wind are present on the scale of radar coverage.

2. Analysis of a nonlinear wind field

As was pointed out before, a harmonic expansion of radial velocity as a function of azimuth is a purely mathematical operation devoid of any physical meaning. The Fourier coefficients can be interpreted physically only when a hypothesis is made on the form of the wind field. We will see now that the assumed form of the wind field imposes also a particular range dependence on the F coefficients. In the case of the linear wind a_1, b_1 must be independent of range and a_0, a_2, b_2 must be linear functions of r. In a more complex form of the wind field the same first five F coefficients will have a different range dependence.

For illustration we will first give in detail the derivation of a new set of equations for a wind with a cubic spatial dependence; that is, a wind field that can be described in terms of its u, v components by

$$u = u_0 + u_x x + u_y y + \tfrac{1}{2}u_{xx}x^2 + u_{xy}xy + \tfrac{1}{2}u_{yy}y^2 + \tfrac{1}{6}u_{xxx}x^3 + \tfrac{1}{2}u_{xxy}x^2y + \tfrac{1}{2}u_{xyy}xy^2 + \tfrac{1}{6}u_{yyy}y^3 \tag{2.1}$$

$$v = v_0 + v_x x + v_y y + \tfrac{1}{2}v_{xx}x^2 + v_{xy}xy + \tfrac{1}{2}v_{yy}y^2 + \tfrac{1}{6}v_{xxx}x^3 + \tfrac{1}{2}v_{xxy}x^2y + \tfrac{1}{2}v_{xyy}xy^2 + \tfrac{1}{6}v_{yyy}y^3. \tag{2.2}$$

Here all the derivatives are evaluated at the center of the scanned circle. For this cubic field, the radial velocity V_r can be written as

$$\begin{aligned} V_r = {} & \frac{r}{2}\left(u_x + v_y + \tfrac{1}{8}u_{xxx}r^2 + \tfrac{1}{8}u_{xyy}r^2 + \tfrac{1}{8}v_{xxy}r^2 + \tfrac{1}{8}v_{yyy}r^2\right) + \left(u_0 + \tfrac{3}{8}u_{xx}r^2 + \tfrac{1}{8}u_{yy}r^2 + \tfrac{1}{4}v_{xy}r^2\right)\sin\beta \\ & + \frac{r}{2}\left(u_y + v_x + \tfrac{1}{4}u_{xxy}r^2 + \tfrac{1}{12}u_{yyy}r^2 + \tfrac{1}{12}v_{xxx}r^2 + \tfrac{1}{4}v_{xyy}r^2\right)\sin2\beta + \left(-\tfrac{1}{8}u_{xx}r^2 + \tfrac{1}{8}u_{yy}r^2 + \tfrac{1}{4}v_{xy}r^2\right)\sin3\beta \\ & + \left(-\tfrac{1}{16}u_{xxy}r^3 + \tfrac{1}{48}u_{yyy}r^3 - \tfrac{1}{48}v_{xxx}r^3 + \tfrac{1}{16}v_{xyy}r^3\right)\sin4\beta + \left(v_0 + \tfrac{1}{4}u_{xy}r^2 + \tfrac{1}{8}v_{xx}r^2 + \tfrac{3}{8}v_{yy}r^2\right)\cos\beta \\ & + \frac{r}{2}\left(v_y - u_x - \tfrac{1}{6}u_{xxx}r^2 + \tfrac{1}{6}v_{yyy}r^2\right)\cos2\beta + \left(-\tfrac{1}{8}v_{xx}r^2 + \tfrac{1}{8}v_{yy}r^2 - \tfrac{1}{4}u_{xy}r^2\right)\cos3\beta \\ & + \left(\tfrac{1}{48}u_{xxx}r^3 - \tfrac{1}{16}u_{xyy}r^3 - \tfrac{1}{16}v_{xxy}r^3 + \tfrac{1}{48}v_{yyy}r^3\right)\cos4\beta. \end{aligned} \tag{2.3}$$

This has the form of a Fourier series up to the fourth-order terms with the first five F coefficients given by

$$a_0 = \frac{r}{2}\left(u_x + v_y + \tfrac{1}{8}u_{xxx}r^2 + \tfrac{1}{8}u_{xyy}r^2 + \tfrac{1}{8}v_{xxy}r^2 + \tfrac{1}{8}v_{yyy}r^2\right)$$

$$a_1 = \left(u_0 + \tfrac{3}{8}u_{xx}r^2 + \tfrac{1}{8}u_{yy}r^2 + \tfrac{1}{4}v_{xy}r^2\right)$$

$$a_2 = \frac{r}{2}\left(u_y + v_x + \tfrac{1}{4}u_{xxy}r^2 + \tfrac{1}{12}u_{yyy}r^2 + \tfrac{1}{12}v_{xxx}r^2 + \tfrac{1}{4}v_{xyy}r^2\right)$$

$$b_1 = \left(v_0 + \tfrac{1}{4}u_{xy}r^2 + \tfrac{1}{8}v_{xx}r^2 + \tfrac{3}{8}v_{yy}r^2\right)$$

$$b_2 = \frac{r}{2}\left(v_y - u_x - \tfrac{1}{6}u_{xxx}r^2 + \tfrac{1}{6}v_{yyy}r^2\right). \quad (2.4)$$

Note that in this case these coefficients do not have a simple physical interpretation. The first five F coefficients contain the same terms as in the analysis of BW with the addition now of higher-order terms. Since the various Fourier harmonics are orthogonal, the addition of the new harmonics in the analysis will not change the numerical values of the first five F coefficients. Their interpretation will change, however, with the number of harmonics needed to represent properly the observations. Let us examine each of these coefficients and their new meaning. The coefficient a_0 in BW's analysis is related to the mean divergence in the scanned circle, which is the mean value of $(u_x + v_y)$. If we compute these derivatives from (2.1) and (2.2) and then evaluate the spatial mean of the sum, that is:

$$(u_x + v_y)_{\text{mean}} = (\nabla \cdot \nabla_h)_{\text{mean}} = \frac{1}{\pi r^2}\int_{\phi}^{2\pi}\int_{\phi}^{r}(u_x + v_y)\,r\,d\theta\,dr \quad (2.5)$$

we find the following expression for the mean horizontal divergence of the cubic wind

$$(\nabla \cdot \nabla_h)_{\text{mean}} = u_x + \tfrac{1}{8}u_{xxx}r^2 + \tfrac{1}{8}u_{xyy}r^2 + v_y + \tfrac{1}{8}v_{yyy}r^2 + \tfrac{1}{8}v_{xxy}r^2. \quad (2.6)$$

This is exactly $2a_0/r$ in (2.4). In fact, the mean divergence over a circle can be obtained from a_0 for any form of the wind field (Rabin and Zawadzki 1984). For a nonlinear wind, however, a_1, b_1, a_2, and b_2 will no longer yield the wind at the origin nor the mean deformation. In the VAD analysis $2a_2/r$, for example, is interpreted as the mean shearing deformation. It can be shown that the mean deformation for a cubic field is

$$(u_y + v_x)_{\text{mean}} = u_y + v_x + \frac{r^2}{8}u_{xxy} + \frac{r^2}{8}u_{yyy} + \frac{r^2}{8}v_{xxx} + \frac{r^2}{8}v_{xyy}, \quad (2.7)$$

which is different from the expression for $2a_2/r$ in (2.4).

Thus, a_2 gives inaccurate information on the mean deformation of the actual wind or the mean deformation of the hypothetical wind. In BW a_1 and b_1 were associated to u_0 and v_0 of the hypothetical linear field. They are sometimes interpreted as the components of the mean wind within the circle of radius r in a nonlinear field. For the cubic wind the actual mean wind is

$$u_{\text{mean}} = u_0 + \tfrac{1}{8}u_{xx}r^2 + \tfrac{1}{8}u_{yy}r^2 \quad (2.8)$$

$$v_{\text{mean}} = v_0 + \tfrac{1}{8}v_{xx}r^2 + \tfrac{1}{8}v_{yy}r^2, \quad (2.9)$$

different from the expressions for a_1 and b_1 in (2.4). It can be also shown that a_1 and b_1 cannot be interpreted either as the mean wind on the perimeter of the circle. Therefore, a linear VAD analysis of a nonlinear wind field will lead to a misinterpretation of all the F coefficients with the exception of a_0. The two coefficients of the first harmonic and the two coefficients of the second harmonic are contaminated by higher-order terms. The observed range dependence of the F coefficients in the case of the cubic wind must obey the polynomials (2.4). Nevertheless, independent of the order of the harmonic analysis needed to represent the observed wind, the first five F coefficients must obey

$$a_0 = \frac{\partial a_1}{\partial r} = a_2 = \frac{\partial b_1}{\partial r} = b_2 = 0 \quad \text{at} \quad r = 0. \quad (2.10)$$

As will be clear from the discussion in the next section, these constraints become very important when the range dependence of an observed F coefficient must be determined.

The question now is whether there is any information, other than mean divergence, that could be retrieved from single-Doppler observations of a nonlinear wind field. From (2.4) we can see that all the F coefficients are range dependent. We will see now how this dependence can be used either to obtain physically meaningful information or at least to test the validity of the hypothesis made on the linearity of the wind field.

3. Development of a VAD analysis for a nonlinear wind

a. Range dependence of the F coefficients

We will now give a general expression for each of the F coefficients that takes into account the order of the truncation in the Taylor expansion used to represent the velocity field (u, v). We saw previously that a cubic field generates up to third-order terms in r in the first five F coefficients. In general, a Taylor expansion of u and v truncated to the order $(m-1)$ can be associated with the first m Fourier harmonics of $V_r(\beta)$, and the highest power of r that appears in the expression of the F coefficients will be $(m-1)$. Also, only terms with odd (even) power in r are present in even (odd) coefficients like $a_0, a_2, b_2 \cdots (a_1, b_1 \cdots)$.

It can be shown that general expression for each of the first five F coefficients are as follows: For a_0, when the highest retained power in the Taylor expansion is $(m-1)$, denoted by a_0^m, the expression is a polynomial of the form

$$a_0^m(r) = \sum_{n=0}^{\eta} A_n r^{2n+1} \tag{3.1a}$$

with $A_0 = (u_x + v_y)/2$, where for $m \geq 2$, $\eta = (m-2)/2$ for an even number of harmonics and $\eta = (m-3)/2$ for an odd number of harmonics. The constants $A_n (n > 0)$ contain the higher-order derivatives of u and v appearing in the Taylor expansion (the exact functional dependence is of no interest here). In the same way

$$a_2^m(r) = \sum_{n=0}^{\eta} B_n r^{2n+1} \tag{3.1b}$$

$$b_2^m(r) = \sum_{n=0}^{\eta} C_n r^{2n+1} \tag{3.1c}$$

with $B_0 = (u_y + v_x)/2$ and $C_0 = (v_y - u_x)/2$. For the odd F coefficients we have the following polynomial expressions:

$$a_1^m(r) = \sum_{n=0}^{\sigma} D_n r^{2n} \tag{3.2a}$$

$$b_1^m(r) = \sum_{n=0}^{\sigma} E_n r^{2n} \tag{3.2b}$$

with $D_0 = u_0$ and $E_0 = v_0$, where $\sigma = (m-1)/2$ for an odd number of harmonics and $\sigma = (m-2)/2$ for an even number of harmonics.

These expressions show that u_0 and v_0 can be obtained from the range dependence of the F coefficients by taking the value of the polynomials $a_1(r)$ and $b_1(r)$ at the origin, and the divergence and deformation at the origin can be obtained by the derivatives of the polynomials for the even coefficients with respect to range at $r = 0$.

b. Height dependence of the F coefficients

Since at very short ranges the Doppler observations are contaminated by ground clutter, particularly for clear-air observations, a fit in range on the observed F coefficients will be necessary to obtain the desired values at the origin. In order to get a valuable fit, a minimum number of observations is needed. On the other hand, in an actual operational situation a compromise has to be made between spatial and temporal resolutions. Thus, for any specific altitude the number of observations may be insufficient to determine unambiguously the range dependence of the coefficients. To partially circumvent this problem we may use the information from the entire volume scan. For this, we introduce in the Taylor expansion the dependence with altitude of the wind components u and v, and modify accordingly the general expressions for the F coefficients. This will, of course, increase the number of terms in the polynomial expressions of these coefficients, but this increase will be greatly offset by the increase of the number of observed values. We use cylindrical coordinates and express V_r as a function of r, β, and z. For low elevations of the radar antenna, the use of cylindrical, instead of spherical, coordinates will not introduce large errors.

Thus, if m harmonics are needed to represent $V_r(\beta)$, the following general polynomial expression is obtained for a_0 as a function of range and height

$$a_0^m(r, z) = \sum_{n=0}^{\eta} \sum_{q=0}^{\zeta} K_{nq} z^q r^{(2n+1)} \tag{3.3}$$

with $K_{00} = (u_x + v_y)/2$, where $\eta = (m-3)/2$ for an odd number of harmonics and $\eta = (m-2)/2$ for an even number of harmonics. The coefficients K_{nq} contain linear combinations of the partial derivatives of u and v with respect to x, y, and z. For a_2 and b_2 we will have the same form of expression, with $(u_x + v_y)$ in K_{00} replaced by $(u_y + v_x)$ for a_2, and by $(v_y - u_x)$ for b_2. Different numerical values of K_{nq} from A_n, etc., will be obtained for the various F coefficients.

For a_1 (and b_1) we have the following polynomial expression:

$$a_1^m(r, z) = \sum_{n=0}^{\sigma} \sum_{q=0}^{\zeta} W_{nq} z^q r^{2n} \tag{3.4}$$

with $W_{00} = u_0$ where $\sigma = (m-1)/2$ for an odd number of harmonics and $\sigma = (m-2)/2$ for an even number of harmonics. The coefficients W_{nq} (hereafter to be called P coefficients) are again linear combinations of the derivatives of u and v at the origin of the coordinates. For b_1, we will have the same expression with $W_{00} = v_0$.

Thus, if $(m-1)$ terms in the Taylor expansion are needed to describe properly a particular wind field, then the single-Doppler observations of this field will be such that m harmonics will be needed to represent $V_r(\beta)$ at

all ranges and the F coefficients will be observed to follow (3.3) and (3.4). That is, the number of harmonics present in the radial velocity as function of azimuth and the order of the polynomials that describe the range dependence of the F coefficients are simply two aspects of the same property of the wind field. The only requirement for the azimuth and range behavior described here is the validity of the hypothesis that the observed wind field can be described by a truncated Taylor series.

c. *Extraction of the information from the F coefficients*

If the inspection of the F coefficients as functions of range reveals strong departures from linearity of the wind field, one could still obtain the wind profile, divergence, shearing, and stretching deformations, all at the center of the coordinates, in the following manner.

(i) At every range and elevation, a least-squares fit is made on V_r to obtain the F coefficients a_0, a_1, b_1, a_2, b_2 for each range and height (these values will be called the "observed" coefficients).

(ii) With the aid of the general expressions (3.3) and (3.4), the truncation order of the polynomials for the F coefficients is determined for the given order of the harmonic analysis.

(iii) Using the result from (ii), a least-squares fit in range and height is made on the values of the observed coefficients a_0, a_1, b_1, a_2, b_2. The purpose of this fit is to determine the values of the P coefficients K_{nq} and W_{nq} in the general expressions (3.3) and (3.4).

(iv) Knowing the values of the K_{nq}, the evaluation of the expressions of a_1 and b_1 at $r = 0$ will give u_0 and v_0. The values of the W_{nq} will enable the evaluation of the derivative of the expressions of a_0, a_2, and b_2 at $r = 0$ leading to the divergence and deformation at the origin. If we allow z to vary while keeping $r = 0$ we will obtain a vertical profile of the considered quantity.

Such an analysis has been done on actual clear-air single-Doppler observations.

4. Observations

The observations were made in Norman, Oklahoma, by the National Severe Storms Laboratory (NSSL) with an S-band radar at eight different elevation angles: 0.4°, 0.8°, 1.2°, 2.0°, 3.0°, 4.0°, 5.0°, and 6.0°. The change in the elevation occurs between azimuth 345° and 360°. The beamwidth is 1° and the Nyquist interval is ± 11 m s^{-1}. Doppler velocities were unfolded by the method described by Zawadzki and Desrochers (1991). Two cases of clear-air data will be discussed here to illustrate the ideas just developed. Although nonlinearities are expected to be of more importance in well-developed precipitation systems, clear-air data avoid the additional difficulty of contamination of radial velocity by the fall speed of precipitation.

In adjusting the observation by the polynomial expressions several considerations must be kept in mind. The analytical expressions for the F coefficients depend on the power at which the Taylor expansion of the wind components is truncated (or equivalently, the order of the associated harmonic analysis needed to represent the VAD). Thus, we must first determine how many terms in the expansion have to be retained to get a good representation of the observed field of V_r. Adding harmonics in the Fourier analysis will improve the quality of the fit made on the observed radial velocities. Also, the adjustment in range of the observed F coefficients by the polynomials will improve with increasing order of the expansion.

Given the antenna program, during the observation used here, there are, at most, three values of the first five F coefficients at each height between the 40- and 100-km range. Thus, with the constraints at the origin (2.10) there are four values (three of which are affected by measurement errors) that can be used to determine the polynomials (3.3) and (3.4). The amount of information is increased to a certain extent by adjusting simultaneously the entire volume scan. In order to account properly for the existing vertical wind shear, however, a sufficiently high-order polynomial in z is required. Thus, there is an upper limit to the maximum value of m, that is, the number of terms in (3.3) and (3.4) that can be determined. Objective tests (chi square and F test) guided our polynomial fits, and it was observed that, for this particular antenna program, there was no improvement in the polynomial adjustments beyond the eight-harmonic representation.

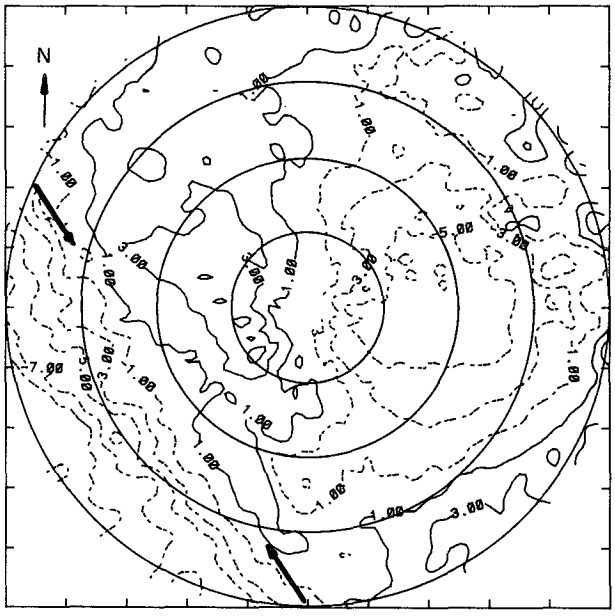

FIG. 1. Radial velocity isolines on the 0.8° elevation antenna scan. A perturbation is seen at 80 km (Rabin et al. 1987). The circles are the 25-, 50-, 75-, and 100-km ranges, respectively.

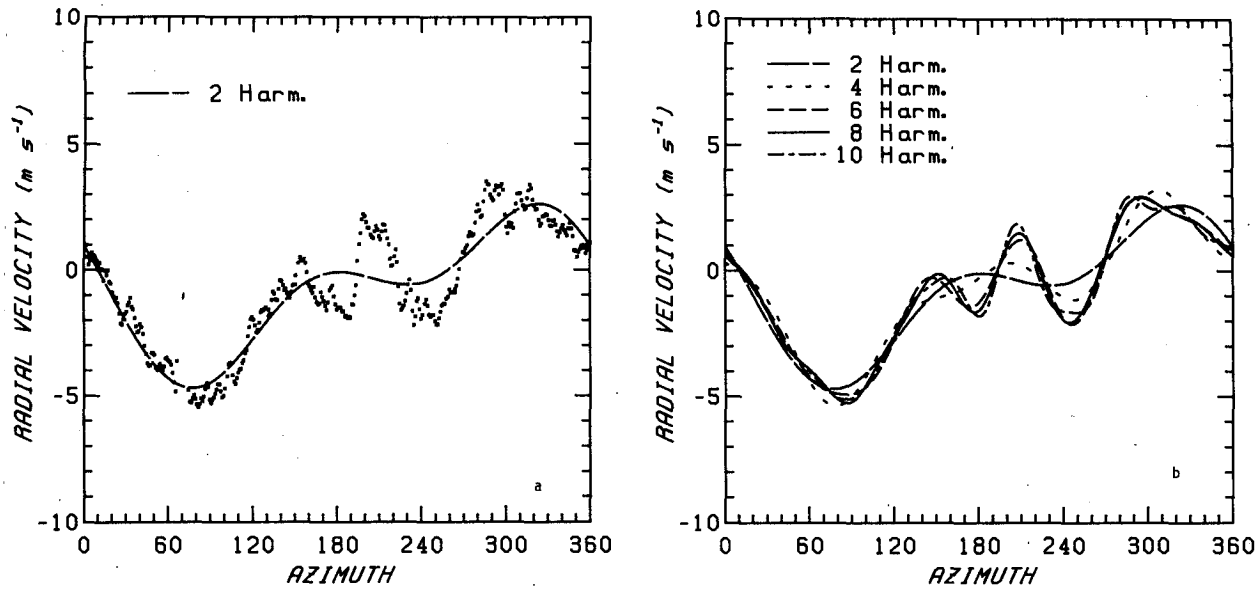

FIG. 2. (a) VAD at r = 53 km and 1.2° elevation. Dots are measured values averaged over a 5° × 4-km region; the curve is the two-harmonic Fourier approximation. (b) Fourier approximations for the VAD in (a) for the indicated number of harmonics.

Inspection of the reflectivity field at all elevations shows that ground clutter completely contaminates the information up to 20 km in range. The contamination is severe between 20 and 30 km and between 30 and 40 km clutter is present over ~45° of azimuth. Because of this, data at $r < 20$ km were rejected, the harmonic analysis of data for $20 < r < 40$ was made eliminating velocities in a ± 1 m s^{-1} interval around the zero values, and the polynomial adjustments were made using data at ranges beyond 40 km only. It should be pointed out, however, that even when ground echoes are not clearly identified, velocity values may be decreased by a weak contribution from fixed targets.

The procedure of analysis described in section 3c was applied in the following manner.

(i) A multiregression linear analysis was used to obtain the F coefficients, as well as their standard deviation, at each range. That is, each term in the Fourier series was considered as an independent variable in a least-squares fit.

(ii) These "observed" F coefficients were adjusted by the polynomials (3.3) and (3.4), using again a multiregression linear analysis (each term in the polynomials was considered as an independent variable). This adjustment was made for various powers of z and various values of m. The standard deviation of the F coefficients was used as weights in the least-squares fit.

Let us first examine data taken on 30 April 1981. The data were collected in clear air in a prestorm environment from 1601:06 to 1610:41 local standard time (LST). Development of convection occurs at the end of the day leading to strong thunderstorms in the scanned area at around 2000 LST. This case was used because a dry front was present in the wind field in the southwest quadrant of the radar-surveyed area. The front is identified by the arrows on the plan position indicator (PPI) display of V_r shown in Fig. 1. The maximum range of the PPI is 100 km. The frontal zone slopes toward the radar and it reaches a height of ~1.5 km at the 40-km range. The perturbation appears to be quite narrow. Thus, while at long ranges the airflow is perturbed over a relatively narrow sector, at ranges closer than 40 km (and above 1.5 km) the flow is affected over most of the azimuth. This case of dry front was described by Rabin et al. (1987), where a more detailed description of the meteorological situation can be found.

As an example, a VAD for the elevation 1.2° at range 53 km is shown in Fig. 2a. The dashed curve, which is the two-harmonic fit, that corresponds to a linear wind approximation is given for reference. The perturbation can be seen at this range in the southwest of the scanned region from azimuth 180° to approximately 300°.

Figure 2b shows the two-, four-, six-, eight-, and ten-harmonic approximation to the VAD of Fig. 2a. Note that the approximation by the Fourier series converges to the observed values; little information remains in the radial velocity beyond the eight-harmonic approximation.

In Fig. 3a the F coefficient a_1 is shown as function of range for the various antenna elevations. The different symbols indicate values at fixed heights. At z = 1.5 km the range dependence of a_1 is negligible; otherwise a_1 is not constant. It decreases with range for

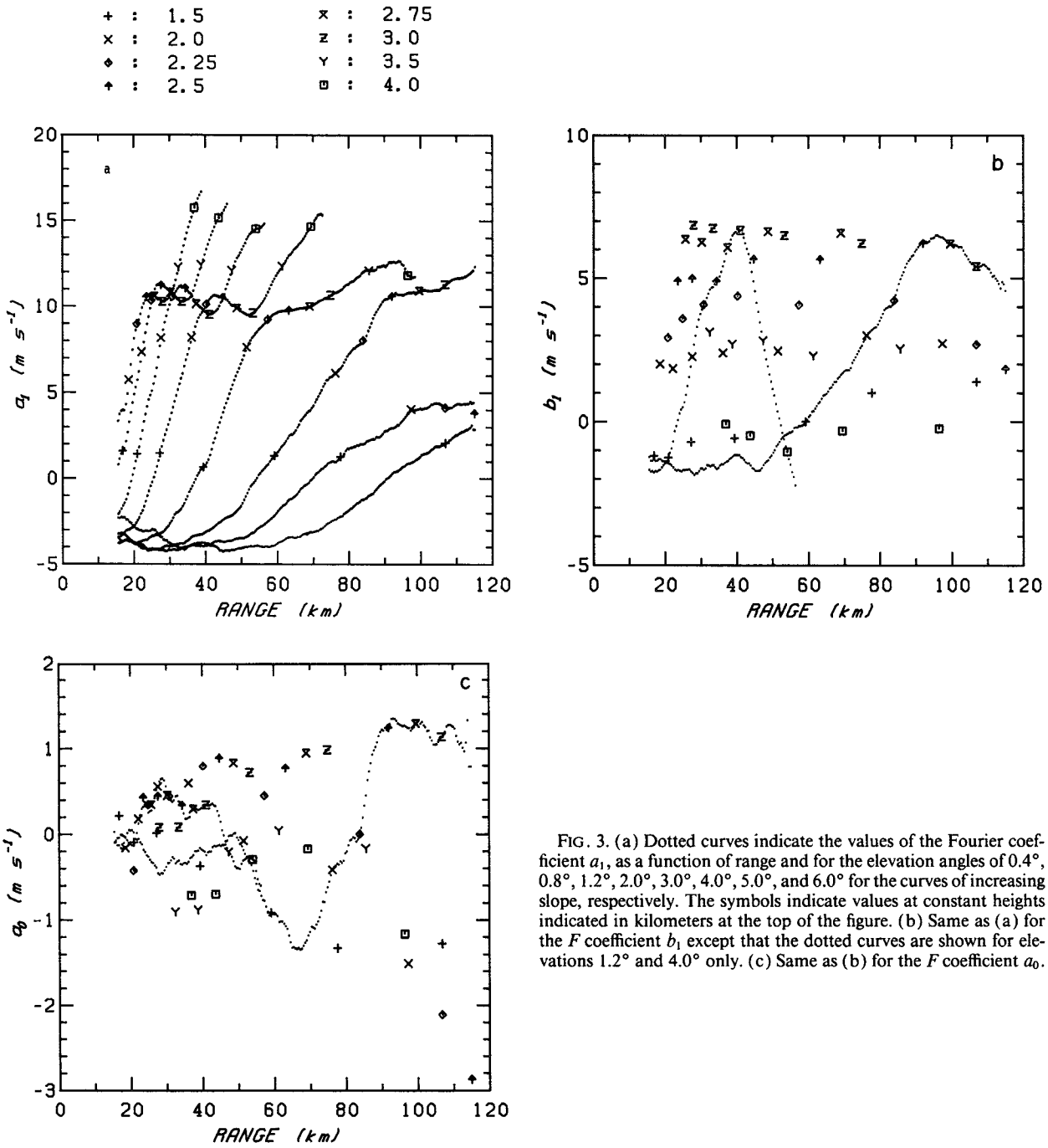

FIG. 3. (a) Dotted curves indicate the values of the Fourier coefficient a_1, as a function of range and for the elevation angles of 0.4°, 0.8°, 1.2°, 2.0°, 3.0°, 4.0°, 5.0°, and 6.0° for the curves of increasing slope, respectively. The symbols indicate values at constant heights indicated in kilometers at the top of the figure. (b) Same as (a) for the F coefficient b_1 except that the dotted curves are shown for elevations 1.2° and 4.0° only. (c) Same as (b) for the F coefficient a_0.

$2.0 < z < 2.5$ km, increases with range for $2.5 < z < 3$ km, is quite constant at 3.5 km, and decreases again at 4.0 km. In Fig. 3b the values of b_1 at constant heights are shown. For clarity the complete set of measurements is shown for two elevations only. Here the dependence with range is weak. This illustrates that a range dependence compatible with the linear wind assumption observed in one F coefficient does not imply that the wind field is actually linear. This is even more apparent in Fig. 3c, where the values of a_0 are shown. For a linear wind a_0 should be a linear function of r with $a_0 = 0$ at $r = 0$. Here the departure from linearity is very strong at 1, 2, and 4 km in height and a_0 is only approximately linear in the 3–3.5-km layer.

Figures 4a–c show the same observations as Figs. 3a–c together with the two-harmonic polynomial adjustments. The adjustments using polynomials that correspond to eight-harmonic analysis are shown in

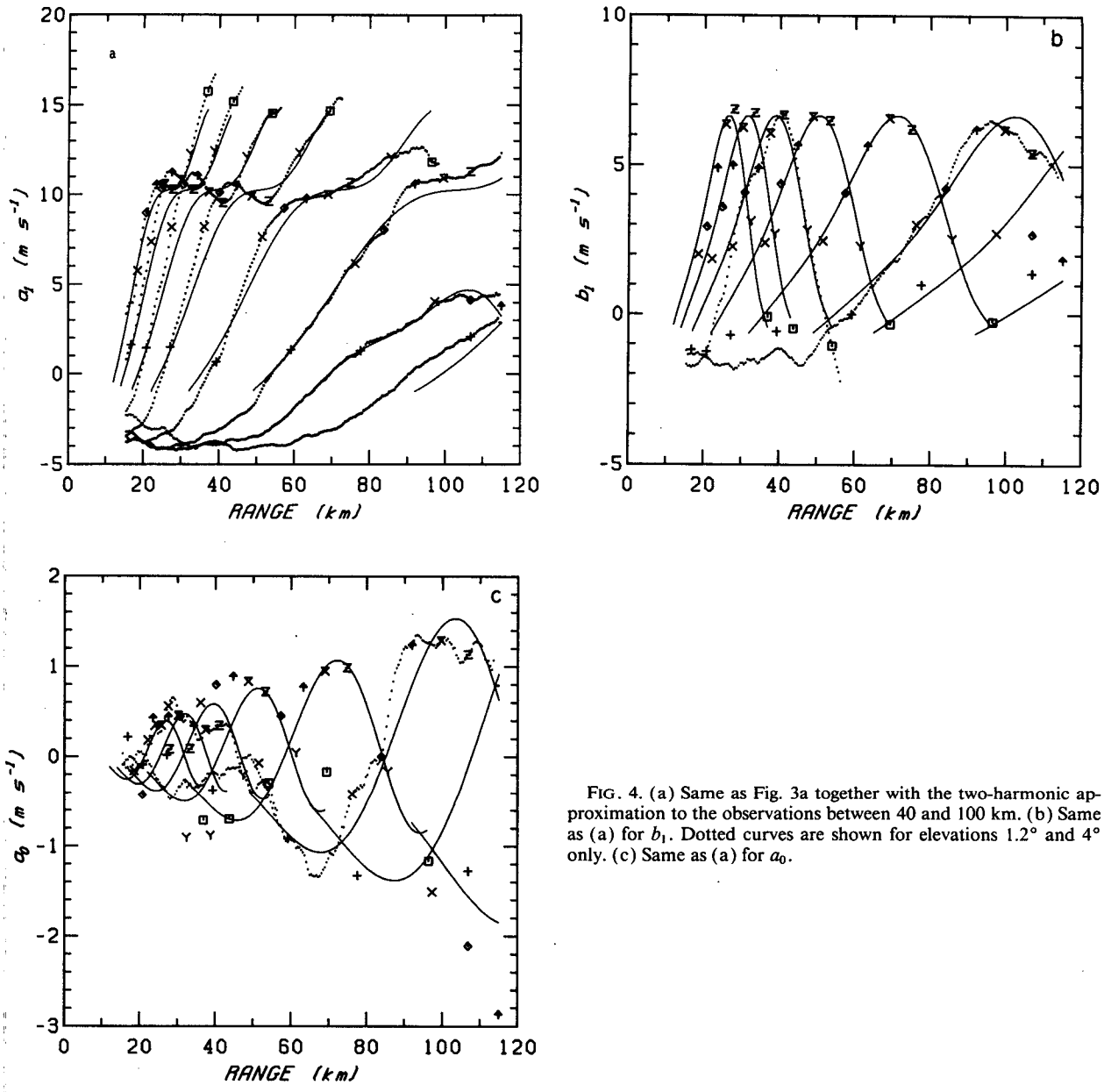

FIG. 4. (a) Same as Fig. 3a together with the two-harmonic approximation to the observations between 40 and 100 km. (b) Same as (a) for b_1. Dotted curves are shown for elevations 1.2° and 4° only. (c) Same as (a) for a_0.

Figs. 5a–c. In all polynomial adjustments only data for $r > 40$ km were used. The highest exponent in the z dependence is 7 in all cases.

Not surprisingly, the polynomials corresponding to the eight-harmonic analysis represent quite better the adjusted observations than does the two-harmonic analysis. It is encouraging to note that, although the observations of a_1 and b_1 between 20 and 40 km were not used to determine the polynomial approximations, they are nevertheless well represented by the eight-harmonic analysis. Furthermore, if the observed values of b_1 at a constant height between the 20- and 40-km ranges are placed on the polynomial approximation curve the resulting behavior with range becomes more consistent with the information at $r > 40$ km. For example, take b_1 at 2.5 km: for $20 < r < 40$ km when the symbols ↑ are shifted upward to reach the polynomial curves the new values fall much closer to the values of b_1 for ranges beyond 40 km, as should be expected from the quasi independence of b_1 with range. This leads us to believe that the discrepancies between the polynomials and the observations of Fig. 5b for $20 < r < 40$ km can be attributed to ground clutter.

For the even F coefficients (a_0, a_2, and b_2) eight-

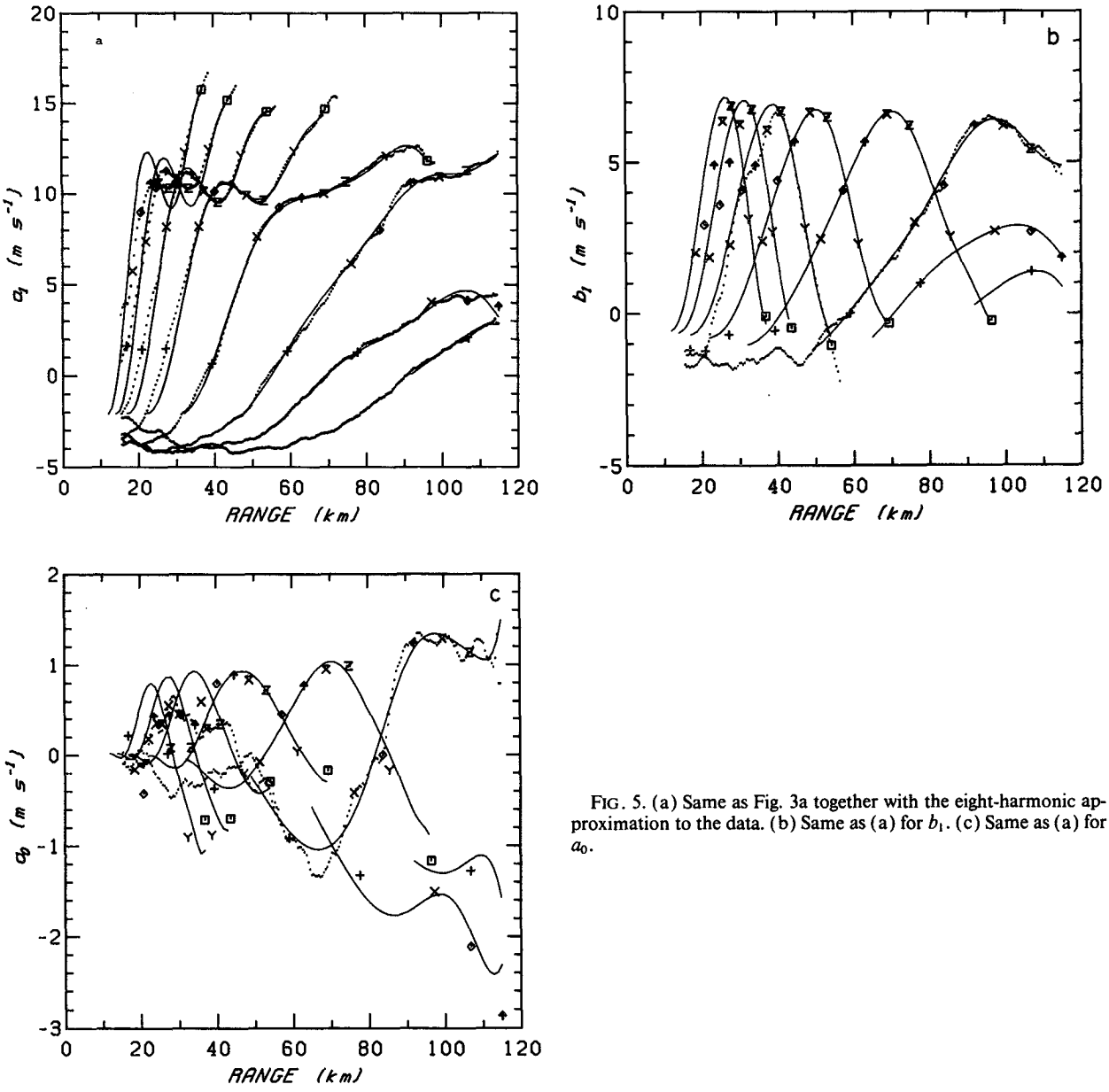

FIG. 5. (a) Same as Fig. 3a together with the eight-harmonic approximation to the data. (b) Same as (a) for b_1. (c) Same as (a) for a_0.

harmonic polynomial adjustment is insufficient to reproduce the more complex range behavior, although there is a marked improvement over the two-harmonic adjustment.

Let us turn our attention to the profiles of the wind components obtained at the origin as described in the preceding section. These profiles are shown in Figs. 6a,b for various approximations to the wind field together with values derived at $r = 35$ km by the VAD analysis for a linear wind.

We have seen that b_1 shows little variation with range at all heights. Thus, it is not surprising to see in Fig. 6b a profile of v_0 that shows little dependence on the order of the polynomial adjustments; this is reassuring inasmuch as it suggests that the measurement errors coupled with the polynomial adjustment method are not generating spurious behavior in the values derived at the origin.

Figure 6a shows the profile of u_0. Again, at levels where a_1 shows little dependence with range (at $\sim$1.5 and $\sim$3.5 km), the values of u_0 obtained by the different polynomial adjustments are very similar. In the 2–3-km layer, however, the differences in the various values of u_0 are appreciable, and one may wonder

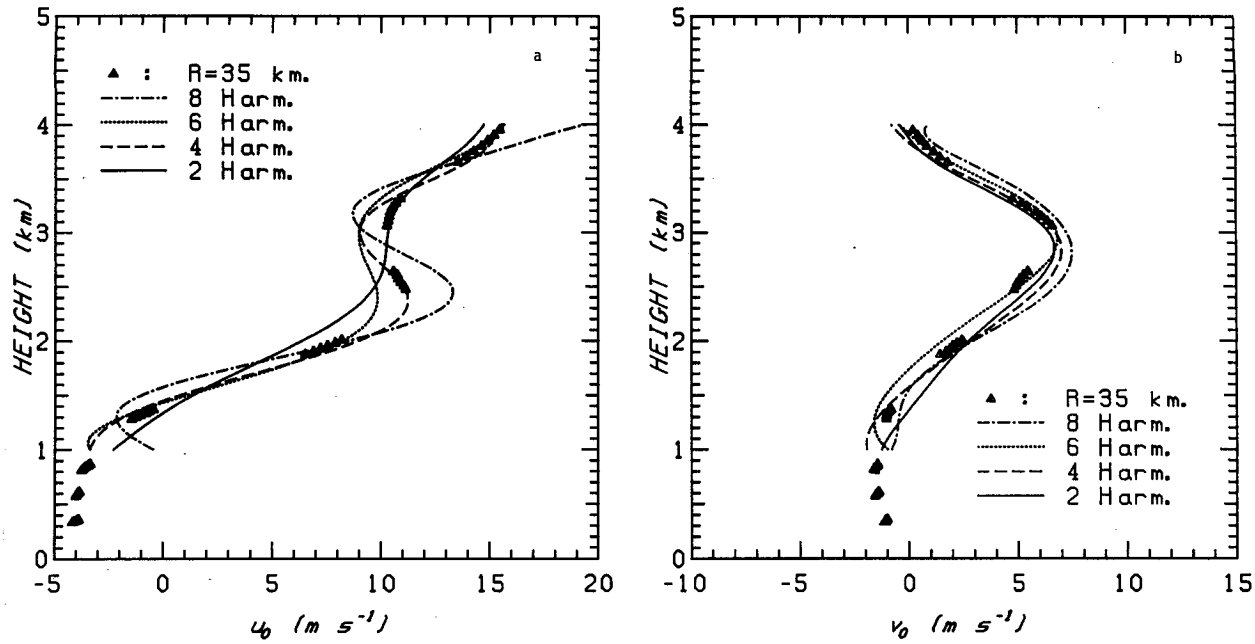

FIG. 6. (a) Profiles of u_0 for the indicated number of harmonics used in the analysis. Also shown are the VAD values of u_0 obtained from data at the 35-km range. (b) Same as (a) for the v_0 wind component.

whether the strong S-shaped variability shown in this layer by the eight-harmonic analysis is real. For lack of an independent measurement we may only point out the consistency of these results with the ensemble of the measurements. In effect, if we turn to Fig. 3a, we notice that the difference in a_1 between 2.5 and 3 km is 1.1 m s^{-1} at around the 70-km distance (fourth antenna elevation), -1.2 m s^{-1} at 50 km (fifth elevation), and -1.8 m s^{-1} at 40 km (sixth elevation). By extrapolation we see that this nonlinear behavior in a_1 is reflected on the S-shaped profile of u_0, showing a difference in a_1 of -4 m s^{-1} between 2.5 and 3 km for the eight-harmonic analysis.

One may wonder if in a frontal situation, such as just described, there is a single wind profile compatible with the entire field of data. Because of this, as a second example, we analyzed a volume scan taken on 19 June 1980 in clear air where no discontinuities in the airflow were apparent. Figure 7a shows the coefficient a_1 as a function of range for the various antenna elevations. The values of a_1 at a fixed height are also indicated by the various symbols. The first overall impression is of a quasi independence of a_1 with range as would be expected for a linear wind. Above 2 km and beyond r = 40 km the variation in a_1 is less than 1 m s^{-1}. For $2 \leqslant z \leqslant 3$ km, however, the coefficient b_1 (Fig. 7b) shows a clear decrease in range of $\sim$4 m s^{-1} between 40 and 108 km in range.

The profiles of u_0 and v_0 are shown in Figs. 8a and 8b, respectively. First, notice that in this case it is u_0 that shows little variation with the order of the polynomial adjustment. Linear VAD analysis at 35 km shows the same values as the eight-harmonic analysis. The nonlinearity of b_1 shown in Fig. 7a is reflected in appreciable variation in values of v_0 depending on the method of analysis.

Although the comparison of the wind components derived by the nonlinear VAD analysis with rawinsonde data is useful and necessary, we should not expect a good agreement between the two, which are of a quite different nature. Contrary to rawinsonde hodograph, the wind profile obtained from Doppler data is truly vertical, it represents the situation prevailing during a few minutes, and it is not affected by local small-scale perturbations. Figures 9a and 9b show the wind components from sonde data obtained on 19 June 1980 at Tuttle (20 km west of the radar) and at Norman at the indicated times. These profiles show a great variability in space and time. The sounding values disagree among themselves by 5 m s^{-1}; that is, as much as the radar velocity components disagree with the soundings. Thus, the latter do not appear to be adequate as truth for the evaluation of the nonlinear VAD analysis of radar data. The radar-derived values should be accepted per se, in view of the soundness of the measurements technique.

We should mention, in passing, that the eight-harmonic analysis of u_0 in Fig. 9a does not show a tendency of decreasing toward low values near the surface as the rawinsonde data do. This illustrates well the danger of freely extrapolating polynomial adjustments outside the information domain. Also, given the antenna ele-

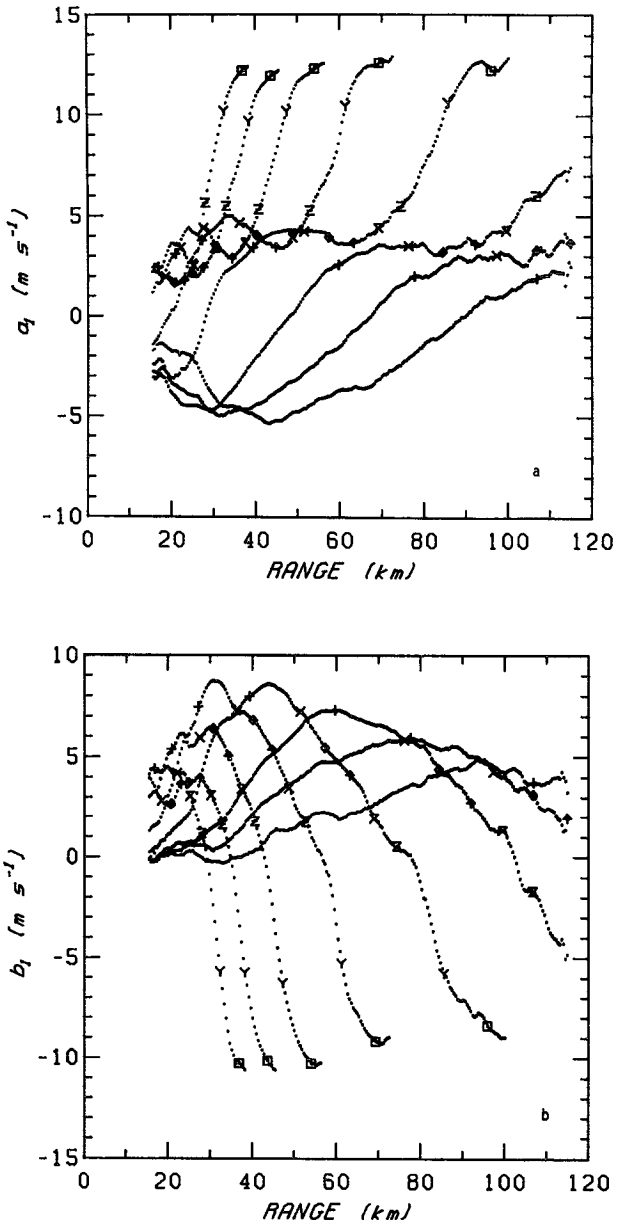

FIG. 7. (a) and (b) Same as Figs. 3a and 3b but for the observations taken on 19 June 1980 (case 2).

vation program, there is a very limited-range extent of data close to the 500-m level, making the polynomial adjustments less reliable at low levels.

5. Discussion

The purpose of this work was to critically examine the commonly accepted assumptions related to the VAD analysis and to better understand certain aspects of single-Doppler observations. We have seen that, when the wind field around the radar site is not linear, the parameters of the VAD analysis at a given range have no clear physical meaning (with the exception of a_0, of course). In particular, a_1 and b_1 give neither the mean wind over or within the circle defined by the constant range, nor the values at the radar site. Moreover, since the best linear fit to the radial component of the wind velocity is not the radial component of the linear part of the wind, it is not possible to give a general and a simple interpretation of the VAD when the observed wind is not linear. It seems intuitive, however, that for weak nonlinearities the error associated with the traditional interpretation of the VAD coefficients should be small.

The range dependence of the coefficients contains information on the degree of nonlinearity. The data analysis shows that, although one of the coefficients may suggest linearity, this may not hold for the other coefficients.

Thus, the VAD analysis must be used judiciously and the range behavior of all the coefficients that are intended for physical interpretation must be verified to be compatible with the linearity of the wind. The analysis of a number of cases at the National Severe Storms Laboratory (NSSL) (Hodl, private communication) suggests that in clear air strong departures from linearity are rare. Nevertheless, the errors in the wind profiling are significant if the nonlinearities are not accounted for.

It has been shown here that a general formulation of the problem of VAD analysis, starting with a Taylor expansion of (u, v) as functions of (x, y), leads to a range dependence of the Fourier coefficients that is represented by polynomials in even powers of range for the odd coefficients and odd powers of range for the even coefficients with constraints on the values or their derivatives at the origin. If observations can be approximated by these polynomials (with the constraints at the origin) it is possible to obtain the desired information on the kinematic properties of the airflow. We have suggested a method for obtaining this information using simultaneously all the information in a volume scan. Our technique should be considered, however, only as a first and tentative exploration. In the two cases analyzed we did not find any objective evidence on a cutoff in the number of harmonics necessary to represent the radial velocity. Although the first two harmonics explain most of the variance in the field of V_r, every additional harmonic contributes, with decreasing importance, to the total variance. Eight harmonics were the maximum allowed by the limited number of elevation scans. It is encouraging that a Fourier expansion in azimuth and polynomials of even or odd powers in range seem to represent adequately values of V_r between 30 and 40 km, although only data beyond 40 km were used to determine the polynomials. This gives some confidence in the profiles of u_0 and v_0

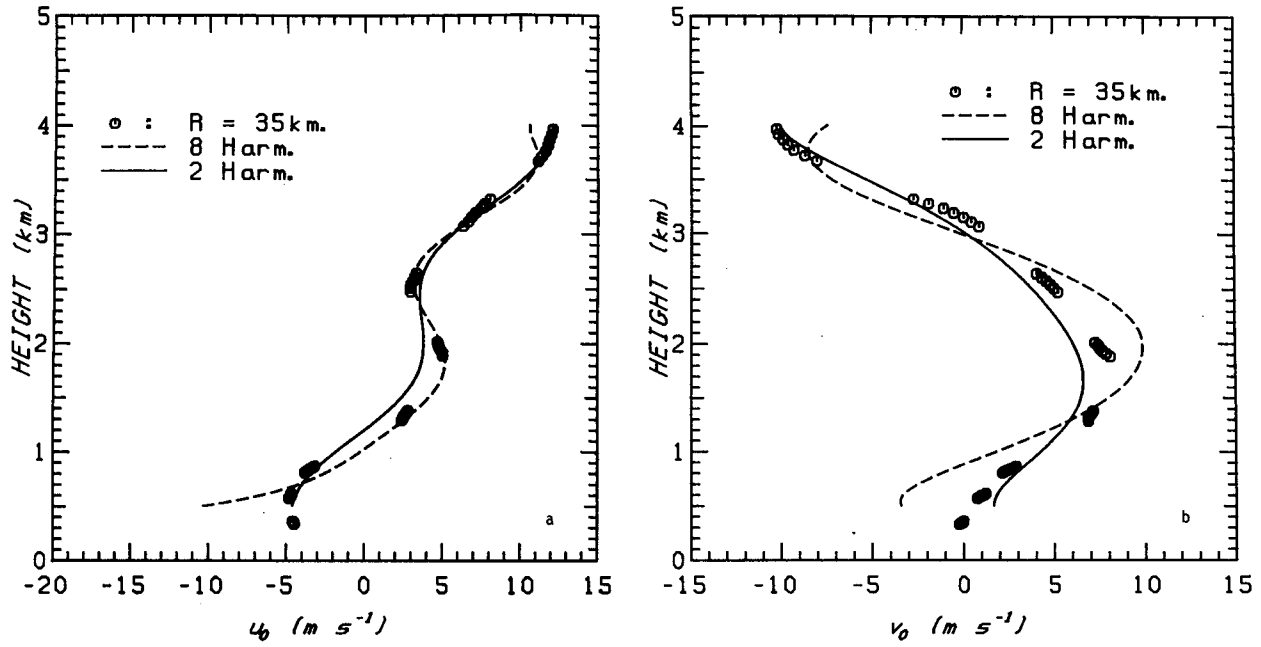

FIG. 8. Same as Figs. 6a and 6b for case 2.

obtained by our technique. In our case the rawinsonde data show too great variability to be used as truth for the profiling with single-Doppler radar. The nature of the two measurements is very different: the rawinsonde gives a wind profile along the trajectory of the balloon; the radar-derived winds give the profile that is compatible with observations over the large area covered by the radar. A number of questions have to be explored before this profiling technique can be accepted with a certain confidence. These questions include up to what

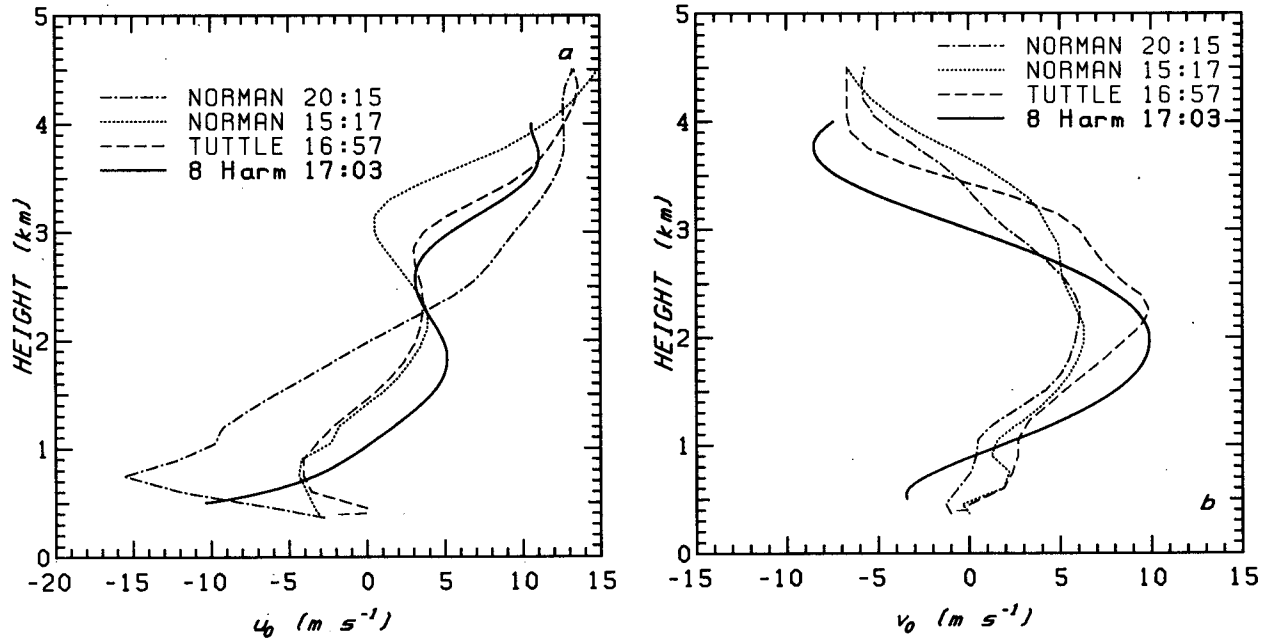

FIG. 9. (a) Profile of u_0 from the eight-harmonic analysis together with rawinsonde data at the indicated times and sites. (b) Same for v_0.

extent wind fields are representable by a Taylor expansion; how many elevations are needed for a good profiling; what the effect is of beam smoothing; etc. For clear-air wind profiling it may be preferable to use scans with high elevation of the antenna so that the ground-clutter problem is minimized and the times when the wind field would be nonlinear would be decreased.

Acknowledgments. This work was partially supported by a grant from the Canadian Atmospheric Environment Service. Data were kindly provided by NSSL. We are indebted to an anonymous reviewer for useful comments and corrections on the manuscript.

REFERENCES

Browning, R. A., and R. Wexler, 1968: The determination of kinematic properties of a wind field using Doppler radar. *J. Appl. Meteor.*, **7**, 105–113.

Easterbrook, C. C., 1973: An area curve fitting method for analysis of Doppler weather radar with application to the study of convectives storms. Calspan Tech. Report No. CK-5077-M-1, 1–34.

Passarelli, R. E., 1983: Wind field estimation by single Doppler radar techniques. *Proc. 21st Weather Radar Conf.*, Boston, Amer. Meteor. Soc., 526–529.

Rabin, R. M., and I. Zawadzki, 1984: On the single Doppler measurements of divergence in clear air. *J. Atmos. and Oceanic Technol.*, **1**, 50–57.

——, D. E. Engles, and A. J. Koscielny, 1987: Application of a Doppler radar to diagnose a frontal zone prior to thunderstorms. *Mon. Wea. Rev.*, **115**, 2674–2686.

Scialom, G., and J. Testud, 1986: Retrieval of horizontal wind field and mesoscale vertical vorticity in stratiform precipitation by conical scannings with two Doppler radars. *J. Atmos. Oceanic Technol.*, **3**, 693–703.

Waldteufel, R., and H. Corbin, 1979: On the analysis of single Doppler data. *J. Appl. Meteor.*, **18**, 532–542.

Zawadzki, I., and C. Desrochers, 1991: A method for real time dealiasing of very moist clear air Doppler data. *Proc. 25th International Conf. on Radar Meteorology.* Boston, Amer. Meteor. Soc., 879–881.